

Article

A Comprehensive Strategy for Accurate Reactive Power Distribution, Stability Improvement, and Harmonic Suppression of Multi-Inverter-Based Micro-Grid

Henan Dong ^{1,2} , Shun Yuan ^{1,3}, Zijiao Han ^{4,*}, Zhiyuan Cai ¹, Guangdong Jia ¹ and Yangyang Ge ²

¹ Institute of Electrical Engineering, Shenyang University of Technology, Shenyang 110023, China; an1an2_nan@163.com (H.D.); yuanshun@serc.gov.cn (S.Y.); mashcaizy@hotmail.com (Z.C.); guangdongjia0302@163.com (G.J.)

² Liaoning Electric Power Company Electric Power Research Institute, State Grid Corporation of China, Shenyang 110006, China; 15942302722@163.com

³ National Energy Administration, Beijing 100085, China

⁴ Liaoning Electric Power Company, State Grid Corporation of China, Shenyang 110004, China

* Correspondence: thuwhatever@163.com; Tel.: +86-139-4047-6382

Received: 10 February 2018; Accepted: 6 March 2018; Published: 26 March 2018

Abstract: Among the issues of accurate power distribution, stability improvement, and harmonic suppression in micro-grid, each has been well studied as an individual, and most of the strategies about these issues aim at one inverter-based micro-grid, hence there is a need to establish a model to achieve these functions as a whole, aiming at a multi-inverter-based micro-grid. This paper proposes a comprehensive strategy which achieves this goal successfully; since the output voltage and frequency of micro-grid all consist of fundamental and harmonic components, the strategy contains two parts accordingly. On one hand, a fundamental control strategy is proposed upon the conventional droop control. The virtual impedance is introduced to solve the problem of accurate allocation of reactive power between inverters. Meanwhile, a secondary power balance controller is added to improve the stability of voltage and frequency while considering the aggravating problem of stability because of introducing virtual impedance. On the other hand, the fractional frequency harmonic control strategy is proposed. It can solve the influence of nonlinear loads, micro-grid inverters, and the distribution network on output voltage of inverters, which is focused on eliminating specific harmonics caused by the nonlinear loads, micro-grid converters, and the distribution network so that the power quality of micro-grid can be improved effectively. Finally, small signal analysis is used to analyze the stability of the multi-converter parallel system after introducing the whole control strategy. The simulation results show that the strategy proposed in this paper has a great performance on distributing reactive power, regulating and stabilizing output voltage of inverters and frequency, eliminating harmonic components, and improving the power quality of multi-inverter-based micro-grid.

Keywords: micro-grid; droop control; virtual impedance; harmonic suppression; power quality

1. Introduction

In recent years, distributed generations, e.g., wind and solar power, have been developing rapidly. Comparing with traditional power generation forms, distributed generations are environment-friendly technologies, and they often form micro-grids via inverters, which is an important complementary of bulk power network. However, since there are so many distributed generations in the micro-grid system, power electronic inverters are also widely used. In addition, various kinds of nonlinear loads

such as electric vehicles are increasingly integrated into the micro-grid, thus a power quality problem inside micro-grid occurs and increases problems of heating, incremental losses, voltage and current distortion, which threaten our daily life. It is not only the micro grid itself that can be broken down by such problems, but the voltage and frequency of the distributed power system can also be influenced through the point of common coupling (PCC) [1–3]. Meanwhile, power management strategies play an increasingly important role in power quality regulation for micro-grids [4–6].

As distributed generations are connected to the micro-grid via inverter, hence the control strategy of inverters influence system stability and power quality. Among all the inverter control strategies, droop control is considered as the best strategy at present, which can distribute the output power of inverters properly under the island mode of the micro-grid, even if there is no common communication line among distributed generations (DGs); meanwhile, the voltage and frequency can be controlled within related national standards by this strategy [7–9]. However, there are some shortcomings in the traditional droop control strategy. Firstly, system reactive power cannot be distributed accurately while the equivalent impedance of micro sources is different [10]. Secondly, system voltage and frequency will not maintain their stability under abrupt load variation [11,12]. In addition, the magnitude of harmonic power varies with the amount of non-linear loads integrated into the micro-grid. The existence of harmonic power will have an effect on system devices, including transformers, capacitors, and electric rotating machines. It is also shown that harmonic power will influence the voltage amplitude and waveform of PCC [13], which may cause resonance and eventually lead to the loss of system stability.

At present, there are less researches on multi-inverter-based micro-grid power quality. Traditional methods for limiting waveforms distortion are to make direct compensation by installing passive or centralized active power filters, but the high cost of these kinds of devices should not be ignored, and these methods can only improve harmonic components, while, as to fundamental component power quality and accurate reactive power distribution, they neither make tense research nor give an integral solution [14–17]. Reference [18] proposed a compensation method based on a unified power quality conditioner (UPQC) to improve the power quality index of PCC, but though this device is widely used in large capacity and high voltage power grids, it is difficult to generalize the use of this device in low voltage distributed grids and micro-grids. Many experts considered designing an inverter control strategy to improve accurate reactive power distribution and govern harmonic components [19–28]. Reference [19] proposed a method to govern harmonic components in the micro-grid that combines the technology of active filter and inverter controller, so the utilization of inverter is obviously improved and the cost of active filter is effectively decreased; however, the design of that controller is too complex to popularize. The general method to distribute reactive power accurately is to add virtual impedances into inverters [20–22]. By measuring the output voltage and current of inverters and adjusting their output impedances, i.e., introducing virtual impedances to the multi-inverter system, the reactive power of system can be distributed accurately, although this method needs to know the parameters of lines in advance and is short of consideration about load variation [23]. Reference [24] concluded that harmonic droop control can be used for distributing harmonic power among inverters and decreasing voltage waveform distortion of PCC, whereas the calculation of non-linear loads is too complex and this method does not make an obvious function on distributing active power. Reference [25] proposed a control strategy to suppress harmonic and negative sequence current in island mode. The strategy mentioned is composed of two controllers: one is a multi-proportional resonance controller which is used to regulate load voltage, and the other is a harmonic impedance controller which is used to distribute harmonic current among micro sources. These two controllers are so intricate that they may lead to high-order feedforward transfer function. In references [26–28], experts considered reactive power distribution, voltage, and frequency stability under load abrupt variation respectively, but the influence from non-linear loads was not taken into integral consideration and given focus in the research.

Above all, this paper proposes a comprehensive strategy for accurate power distribution, stability improvement and harmonic suppression of a multi-inverter-based micro-grid, which aims at further

improving the power quality of the micro-grid. Based on previous research, it mainly introduces the improved fundamental control strategy and the fractional frequency harmonic control strategy into a multi-inverter-based micro-grid, which are two components of the comprehensive strategy. The key point is to add the fractional frequency harmonic control strategy to improve the power quality of the multi-inverter-based micro-grid under the premise of ensuring the stability of the improved fundamental control strategy. In addition, the stability of this micro-grid control system is analyzed by the small signal analysis method. Following this, a micro-grid system simulation model is built in MATLAB to verify the effectiveness of the proposed strategy.

The main contributions of this work are described as follows: Section 2 proposes the comprehensive strategy for accurate power distribution, stability improvement, and harmonic suppression of the multi-inverter-based micro-grid. Section 3 analyzes the stability of the multi-converter parallel system after introducing the comprehensive control strategy. Simulation and experimental results to prove the effectiveness of the strategy are demonstrated in Section 4. Section 5 concludes the paper.

2. Comprehensive Strategy for Accurate Reactive Power Distribution, Stability Improvement, and Harmonic Suppression of a Multi-Inverter-Based Micro-Grid

It is difficult to accurately distribute reactive power and effectively improve the stability of voltage and frequency under abrupt load variation depending on conventional droop controllers, let alone suppress harmonic components in a micro-grid which are caused by many reasons. Therefore, a comprehensive strategy for accurately distributing reactive power, improving stability, and suppressing harmonics of a multi-inverter-based micro-grid is proposed in this paper. Upon the conventional droop control, an adaptive virtual impedance control loop is introduced to achieve the accurate distribution of reactive power of inverters in fundamental frequency. Considering this process may add the problem of voltage stability, so a secondary power balance controller is added to improve the stability of voltage and frequency, and the fundamental problems are settled completely so far. Next, the control strategy this paper proposed is further refined by introducing a fractional frequency harmonic suppression strategy, which can solve the harmonic problem perfectly, therefore, the power quality of the micro-grid is improved eventually.

The main circuit is mainly composed of the following parts: inverter, LC filter, line impedance, linear load, nonlinear load, and so on. The inverter is controlled by a control strategy to adjust the output voltage and frequency. The comprehensive control strategy is composed of the improved fundamental control strategy and fractional frequency harmonic control strategy.

The improved fundamental control strategy is proposed upon the conventional droop control, and the problem of accurate reactive power distribution is solved by introducing virtual impedance to inverters. The secondary power balance controller is added to improve the stability of voltage and frequency. The reference value of the frequency is 50 Hz and the reference value of the output voltage is 311 V in secondary power balance controller. The voltage value and frequency of the PCC follow a given value through the closed loop control strategy.

The fractional frequency harmonic control strategy is proposed to solve the influence of nonlinear loads, micro-grid inverters, and the distribution network on output voltage of inverters, which is focused on eliminating specific harmonics caused by the nonlinear loads, micro-grid converters, and the distribution network, so the power quality of micro-grid can be improved effectively. The 5th harmonic suppression is taken as an example. Firstly, the 5th harmonic voltage and 5th harmonic current of the PCC are detected, and the harmonic power is calculated. The reference value of the output voltage of the inverter and frequency are generated according to the droop curve of the harmonic. The closed loop control strategy is adopted in the reference value and the detection value of PCC, so that the output value of the harmonic is followed by a given value, which is 0, and the 5th harmonic is eliminated. The way to suppress other harmonics is the same as the 5th harmonic. The main control block diagram is shown in Figure 1.

In Figure 1, L_f is the filter inductance; R_f is the filter resistance; C_f is the filter capacitance; R_{line} is the line resistance; L_{line} is the line inductance; R_{ref} is the reference resistance; X_{ref} is the reference reactance; R_i is the calculated value of line resistance, X_i is the calculated value of line inductance; P_{line} is the line active power; Q_{line} is the line reactive power; P_{i_LPF} is the active power that passes through the low pass filter; Q_{i_LPF} is the reactive power that passes through the low pass filter; E^* is an reference voltage; f^* is an reference frequency; E_{nh} is the nth harmonic voltage; P_{nh} is the active power of the nth harmonic; and Q_{nh} is the reactive power of the nth harmonic.

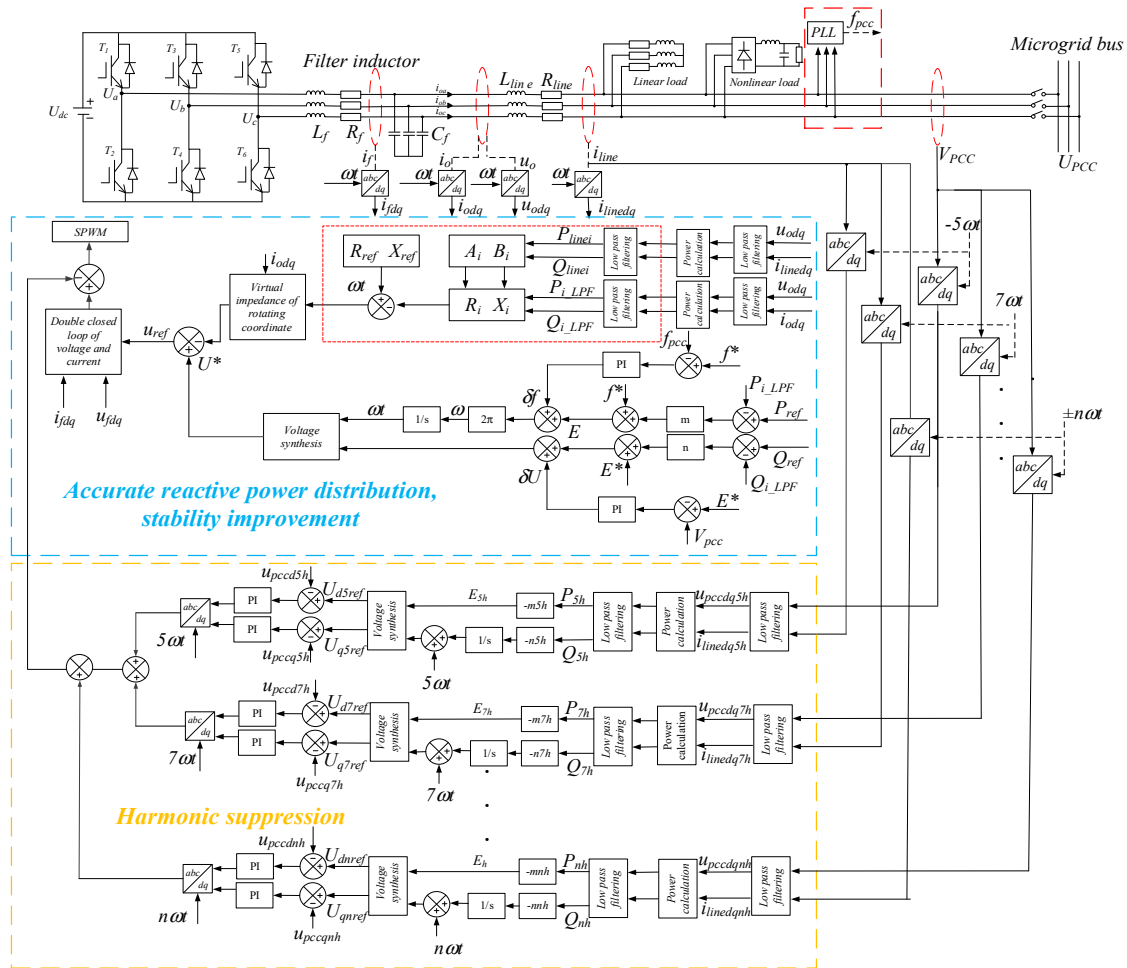


Figure 1. Block diagram of comprehensive control strategy.

2.1. Combination of Adaptive Virtual Impedance Drooping Control and Secondary Power Balance Control Strategy

In order to achieve an accurate distribution of reactive power of inverters, an adaptive virtual impedance control loop is introduced upon conventional droop control. The control block diagram is shown in Figure 2.

The output voltage function of the inverter with virtual impedance is:

$$U_0(s) = G(s)U_{ref}(s) - [G(s)Z_v(s) + Z_{eq}(s)]I_0(s). \tag{1}$$

The output power values of the inverter can be calculated by

$$P_i = \frac{U_i}{R_i^2 + X_i^2} [R_i(U_i - E \cos \delta_i) + X_i E \sin \delta_i] \tag{2}$$

$$Q_i = \frac{U_i}{R_i^2 + X_i^2} [-R_i E \sin \delta_i + X_i (U_i - E \cos \delta_i)] \quad (3)$$

where: R_i and X_i are the power equivalent output resistance and reactance, respectively, which is defined by inverter output power and the power injected to the PCC. Z_v is virtual impedance.

Based on the above circuit, the transmission line parameters and loads fluctuation will affect the value of power equivalent impedance, then influence the reactive power distribution. The power equivalent impedance can be calculated through line power.

$$U_i(U_i - U \cos \delta_i) = P_{linei} R_{linei} + Q_{linei} X_{linei} = A_i \quad (4)$$

$$U_i U \sin \delta_i = P_{linei} X_{linei} - Q_{linei} R_{linei} = B_i \quad (5)$$

and the inverter equivalent output impedance can be obtained by

$$R_i = \frac{P_i A_i + Q_i B_i}{P_i^2 + Q_i^2} \quad (6)$$

$$X_i = \frac{P_i B_i - Q_i A_i}{P_i^2 + Q_i^2} \quad (7)$$

then the virtual impedance of each micro source is calculated by

$$R_{vi} = R_{ref} - R_i \quad (8)$$

$$X_{vi} = X_{ref} - X_i. \quad (9)$$

The adaptive virtual impedance control strategy can accurately distribute reactive power, meeting the requirement of the power decoupling and stability margin. The meaning of adaptive is that the virtual impedance varies along with the power equivalent output impedance when the loads change, and it can also be changed if the micro-grid central controller changes reference impedance.

The traditional droop control can realize automatic regulation of P/f and Q/V , the essence of which, however, is a kind of deviating regulation. Considering the addition of the virtual impedance will increase the degree of deviation, which is harmful to the voltage stability. Therefore, a secondary power balance control strategy is added to stabilize the output voltage of converters, as well as improve the stability of frequency. The compensation frequency and voltage of this strategy can be derived by Equations (10) and (11):

$$\delta f = k_{p\omega}(f^* - f) + k_{i\omega} \int (f^* - f) dt \quad (10)$$

$$\delta U = k_{pE}(U^* - U) + k_{iE} \int (U^* - U) dt \quad (11)$$

where: f^* and f are rated frequency and operational frequency of the microgrid, respectively; U^* and U are rated voltage and operational voltage, respectively. The frequency compensation signal δf and voltage compensation signal δU obtained from the secondary power balance controller are sent to each micro source, then the droop curves of micro sources will turn to be appropriate translations, then the voltage and frequency can be stabilized by adding this strategy, which is similar to the secondary frequency modulation of thermal power unit. Until now, not only can the reactive power be distributed accurately, but also the stability of voltage and frequency can be improved effectively, hence the combination of adaptive virtual impedance drooping control and secondary power balance control strategy in fundamental frequency is achieved completely.

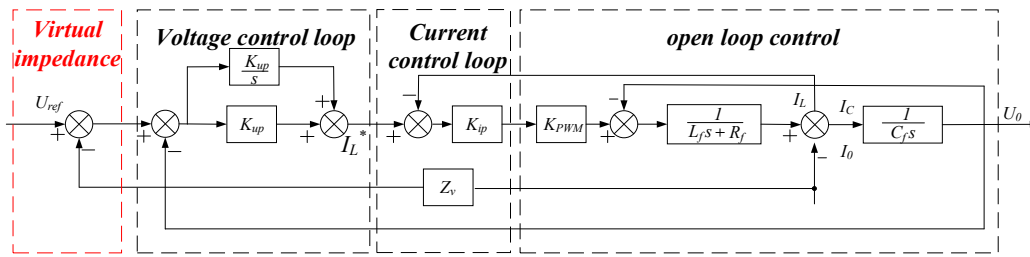


Figure 2. Inverter control block diagram with virtual impedance.

2.2. Fractional Frequency Harmonic Drooping Control Strategy

According to the circuit superposition theorem, a linear circuit with different frequencies can be analyzed separately at each frequency. Reference [29] confirmed that any harmonic, e.g., the h th harmonic can be extracted for separate analysis and control when the whole system enters steady state, so the harmonic droop control strategy is proposed to eliminate the 5th, 7th, 11th, and 13th harmonics generated by nonlinear loads. In order to reduce the harmonic voltage of the system, the harmonic voltage compensation value is calculated by the harmonic droop control strategy. The system equivalent schematic is shown in Figure 3.

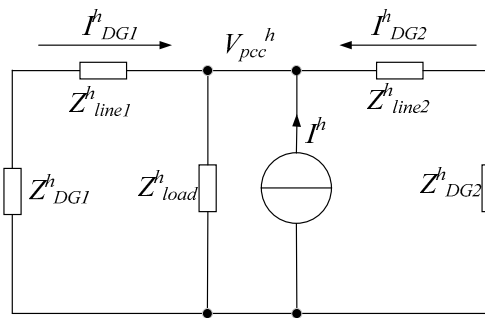


Figure 3. System equivalent circuit containing different frequencies.

In order to make the harmonic voltage of the inverter reach or close to zero, the V_{oh} should be zero, and the load part of the harmonic equivalent circuit can be equivalent to a current source [30], then the output voltage of inverter can be obtained:

$$\bar{V}_o = E \angle \delta - Z_o I \angle \theta = E \cos \delta - Z_o I \cos \theta + j(E \sin \delta - Z_o I \sin \theta). \quad (12)$$

The phase angle difference δ is the phase angle difference between the voltage source and the current source. When it is very small, Equations (13) and (14) can be obtained:

$$P \approx EI - Z_o I^2 \cos \theta \quad (13)$$

$$Q \approx EI \delta - Z_o I^2 \sin \theta. \quad (14)$$

From Equations (13) and (14), it can be found that whether the impedance of the line is inductive, resistive, or capacitive, the correlation between P and E , and Q and δ , can be concluded. Thus the h th harmonic droop controller can be shown as:

$$E_h = E^* - n_h P_h \quad (15)$$

$$\omega_h = \omega^* - m_h Q_h \quad (16)$$

where: P_h and Q_h are the calculated values of active power and reactive power under the h th harmonic frequency; n_h and m_h are the corresponding h th harmonic droop coefficients; E_h is the RMS of the h th harmonic voltage; and ω_h is the h th harmonic voltage angle frequency. The amplitude and angular frequency of specific harmonic voltage can be eliminated by this control strategy, and the reference value of harmonic voltage on the dq axis can be obtained through voltage synthesis and coordinate transformation. The modulated wave is used to turn on and turn off the inverter switch tube so as to produce the appropriate output voltage, so the PCC harmonic voltage can be suppressed effectively. The structure diagram of the harmonic drooping control is shown in Figure 4.

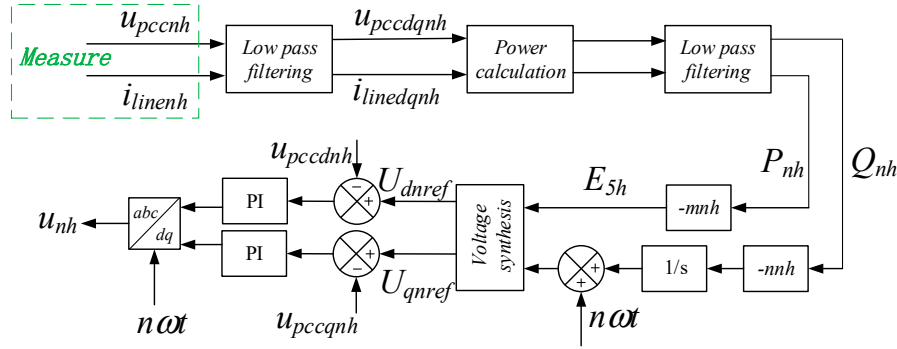


Figure 4. Harmonic drooping control structure.

3. Stability Analysis of the Multi-Converter Parallel System after Introducing the Comprehensive Control Strategy

In this section, a small signal analysis method is used to verify the effectiveness of the control strategy. The small signal analysis model of the single inverter is shown as follows (17):

$$\begin{aligned} [\Delta \dot{x}_{invi}] &= A_{invi}[\Delta x_{invi}] + B_{invi}[\Delta v_{bDQi}] + B_{iwcom}[\Delta \omega_{com}] \\ \begin{bmatrix} \Delta \omega_i \\ \Delta i_{odqi} \end{bmatrix} &= \begin{bmatrix} C_{INV\omega i} \\ C_{INVci} \end{bmatrix} [\Delta x_{invi}] \end{aligned} \tag{17}$$

where:

$$\begin{aligned} A_{invi} &= \begin{bmatrix} A_{pi} & 0 & 0 & 0 & B_{pi} \\ 0 & A_{vi} & 0 & 0 & B_{vi} \\ B_{u1i}D_{vi}C_{pui} & B_{u1i}C_{vi} & 0 & 0 & B_{u2i} \\ B_{c1i}D_{u1i}D_{vi}C_{pui} & B_{c1i}D_{u1i}C_{vi} & B_{c1i}C_{ui} & 0 & B_{c1i}D_{u2i} + B_{c2i} \\ B_{LC1i}D_{C1i}D_{u1i}D_{vi}C_{pui} + B_{LC2i}T_u + B_{LC3i}C_{pui} & B_{LC1i}D_{c1i}D_{u1i}C_{ui} & B_{LC1i}D_{c1i}D_{u1i}C_{ui} & B_{LC1i} + C_{ci} & A_{LCi} + B_{LC1i}D_{c1i}D_{u2i} \end{bmatrix} \\ B_{invi} &= \begin{bmatrix} 0 & 0 & 0 & B_{LC3i}T_s^{-1} \end{bmatrix}_{15 \times 2}^T \\ B_{iwcom} &= \begin{bmatrix} B_{pwcom} & 0 & 0 & 0 \end{bmatrix}_{15 \times 1}^T \\ C_{inv\omega i} &= \begin{cases} \begin{bmatrix} C_{p\omega} & 0 & 0 & 0 \end{bmatrix}_{1 \times 15} & i = 1 \\ \begin{bmatrix} 0 & 0 & 0 & 0 \end{bmatrix}_{1 \times 15} & i \neq 1 \end{cases} \\ C_{invci} &= \begin{bmatrix} T_i & 0 & 0 & T_s \end{bmatrix} \end{aligned} \tag{18}$$

A single inverter model is augmented in $i = 2$. The first inverter is used as the angle reference, so that the small signal model of two inverters can be obtained:

$$\begin{aligned} [\Delta \dot{x}_{inv}] &= A_{inv}[\Delta x_{inv}] + B_{inv}[\Delta v_{bdq}] \\ [\Delta i_{odq}] &= C_{invci}[\Delta x_{inv}] \end{aligned} \tag{19}$$

where:

$$A_{inv} = \begin{bmatrix} A_{inv1} + B_{1\omega com}C_{inv\omega1} & 0 \\ 0 & A_{inv2} + B_{2\omega com}C_{inv\omega1} \end{bmatrix} \tag{20}$$

$$B_{inv} = \begin{bmatrix} B_{inv1} \\ B_{inv2} \end{bmatrix}; C_{invc} = \begin{bmatrix} C_{invc1} & 0 \\ 0 & C_{invc2} \end{bmatrix}; C_{inv\omega} = \begin{bmatrix} C_{inv\omega1} & C_{inv\omega2} \end{bmatrix}$$

where: Δx_{inv} is the state variable of the inverter; A_{inv} is the state matrix of the inverter; Δv_{bdq} is the outlet voltage of the inverter; $\Delta \omega_{com}$ is a common angular frequency; B_{inv} and $B_{\omega com}$ are the input matrix of the inverter; $\Delta \omega$ is the angle frequency of the inverter; Δi_{odq} is the output current of the inverter; and $C_{inv\omega}$ and C_{invc} are the output matrices of the inverter.

The load is equivalent to the form of RL series for the micro-grid model, and its equivalent model is:

$$\dot{[\Delta i_{loaddq}]} = A_{load} [\Delta i_{loaddq}] + B_{1load} [\Delta u_{bdq}] + B_{2load} \Delta \omega \tag{21}$$

in which:

$$A_{load} = \begin{bmatrix} -\frac{R_{load}}{L_{load}} & \omega_0 \\ -\omega_0 & -\frac{R_{load}}{L_{load}} \end{bmatrix} \tag{22}$$

$$B_{1load} = \begin{bmatrix} \frac{1}{L_{load}} & 0 \\ 0 & \frac{1}{L_{load}} \end{bmatrix}; B_{2load} = \begin{bmatrix} I_{loadq} \\ I_{loadd} \end{bmatrix}$$

where: R_{load} is load equivalent resistance, L_{load} is load equivalent reactance, and I_{loaddq} is load current.

In order to express the load-containing microgrid system in the form of state matrix, the virtual parameter r_n is introduced to replace the input of the original state space expression.

$$\begin{cases} u_{bd} = r_n(i_{od} - i_{loadd}) \\ u_{bq} = r_n(i_{oq} - i_{loadq}) \end{cases} \tag{23}$$

Therefore, the small signal model of the fundamental wave of the inverter model is as follows:

$$\dot{\Delta x_{mg}} = A_{mg} \Delta x_{mg} \tag{24}$$

in which:

$$A_{mg} = \begin{bmatrix} A_{inv} + B_{inv}R_nC_{invc} & -B_{inv}R_n \\ B_{1load}R_nC_{invc} + B_{2load}C_{inv\omega} & A_{load} - B_{1load}R_n \end{bmatrix} \tag{25}$$

$$\Delta x_{mg} = \begin{bmatrix} \Delta \delta_1 & \Delta P_1 & \Delta Q_1 & \Delta X_{1dq} & \Delta \phi_{1dq} & \Delta \gamma_{1dq} & \Delta i_{1dq} & \Delta v_{o1dq} & \Delta i_{o1dq} & \Delta \delta_2 \\ \Delta P_2 & \Delta Q_2 & \Delta X_{2dq} & \Delta \phi_{2dq} & \Delta \gamma_{2dq} & \Delta i_{2dq} & \Delta v_{o2dq} & \Delta i_{o2dq} & \Delta i_{loaddq} \end{bmatrix} \tag{26}$$

where: Δx_{mg} is the state variable of the inverter, and ΔA_{mg} is the state matrix of the inverter.

The block diagram of the harmonic droop control is shown in Figure 5.

The harmonic droop control structure contains the harmonic power calculation module, the low pass filter module, and the harmonic droop module, which is similar to the fundamental droop control structure. The small signal model of harmonic power droop controller can be written as the form of state space function, and the expression of state space expression are:

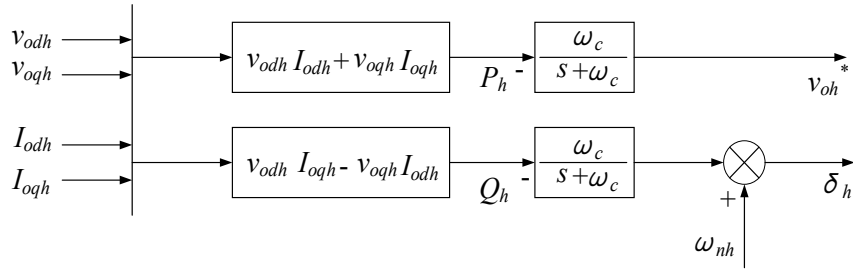


Figure 5. Harmonic droop control block diagram.

$$\begin{bmatrix} \dot{\Delta\delta_h} \\ \Delta P_h \\ \Delta Q_h \end{bmatrix} = A_{mgh} \begin{bmatrix} \Delta\delta_h \\ \Delta P_h \\ \Delta Q_h \end{bmatrix} + B_{mgh} \begin{bmatrix} \Delta i_{ldqh} \\ \Delta v_{odqh} \\ \Delta i_{odqh} \end{bmatrix} + B_{mg\omega h} \Delta\omega_{comh} \quad (27)$$

$$\begin{bmatrix} \Delta\omega_h \\ \Delta v_{odqh}^* \end{bmatrix} = \begin{bmatrix} C_{mg\omega h} \\ C_{mgvh} \end{bmatrix} \begin{bmatrix} \Delta\delta_h \\ \Delta P_h \\ \Delta Q_h \end{bmatrix} \quad (28)$$

in which:

$$A_{mgh} = \begin{bmatrix} 0 & 0 & -m_h \\ 0 & -\omega_c & 0 \\ 0 & 0 & -\omega_c \end{bmatrix} \quad B_{mg\omega h} = \begin{bmatrix} -1 \\ 0 \\ 0 \end{bmatrix} \quad (29)$$

$$B_{mgh} = \begin{bmatrix} 0 & 0 & 0 & 0 & 0 & 0 \\ 0 & 0 & \omega_c I_{odh} & \omega_c I_{oqh} & \omega_c V_{odh} & \omega_c V_{oqh} \\ 0 & 0 & \omega_c I_{oqh} & -\omega_c I_{odh} & -\omega_c V_{oqh} & \omega_c V_{odh} \end{bmatrix}$$

$$C_{mg\omega} = \begin{bmatrix} 0 & 0 & -m_h \end{bmatrix} \quad C_{mgvh} = \begin{bmatrix} 0 & -n_h & 0 \\ 0 & 0 & 0 \end{bmatrix}$$

where v_{odh} and v_{oqh} represent the output harmonic voltages of inverter under dq coordinate system; i_{odh} and i_{oqh} represent the output harmonic currents of inverter under dq coordinate system; P_h is the h th harmonic active power; Q_h is the h th harmonic reactive power; ω_c represents the cut-off frequency of the low pass filter; m_h and n_h represent the reactive and active power drooping coefficients; ω_h is the h th harmonic angular frequency; ω_{comh} is the common angular frequency under the h th harmonic coordinate system; and δ_h is the h th harmonic angle.

The linearization of harmonic drooping voltage loop is the same as fundamental linearization.

The state space model of the harmonic droop control strategy in the multi-inverter-based micro-grid is:

$$\dot{\Delta x_{mgh}} = A_{mgh} \Delta x_{mgh} \quad (30)$$

$$\Delta x_{mgh} = \begin{bmatrix} \Delta\delta_h & \Delta P_h & \Delta Q_h & \Delta\phi_{dq} & \Delta i_{ldqh} & \Delta v_{odqh} & \Delta i_{odqh} & \Delta i_{loaddqh} \end{bmatrix}. \quad (31)$$

The state space model of the comprehensive control strategy in the multi-inverter-based micro-grid is:

$$\dot{\Delta x_{mga}} = A_{mga} \Delta x_{mga} \quad (32)$$

$$\dot{\Delta x_{mga}} = \begin{bmatrix} \dot{\Delta x_{mg}} \\ \dot{\Delta x_{mgh}} \end{bmatrix} \quad \Delta x_{mga} = \begin{bmatrix} \Delta x_{mg} \\ \Delta x_{mgh} \end{bmatrix} \quad A_{mga} = \begin{bmatrix} A_{mg} & 0 \\ 0 & A_{mgh} \end{bmatrix} \quad (33)$$

where: x_{mg} is the state variable under fundamental frequency; i_{loaddq} is a load fundamental current; A_{mg} is a fundamental state matrix; x_{mgh} is the state variable under the h th harmonic frequency; $i_{loaddqh}$ is the h th harmonic load current; A_{mgh} is the h th harmonic state matrix; x_{mga} is the comprehensive state variable under all frequencies; and A_{mga} is the comprehensive state matrix.

The stability simulation of the control strategy is carried out, in which the line resistance is 0.0428Ω and the line inductance is 2.8 mH . The active droop coefficient $m_p = 1 \times 10^{-5}$ and the reactive droop coefficient $n_q = 3 \times 10^{-5}$. In the improved fundamental control strategy, the filter inductance is 0.6 mH , the filter capacitor is 1.5 mF , $P = 1$, $I = 2$ in PI parameters of voltage, $P = 5$ in PI parameters of current. In the fractional frequency harmonic control strategy, the active droop coefficient is -0.01361 , the reactive power droop coefficient is -0.2609 , $KI = 10$, $PI = 50$ in the voltage closed loop.

The stability analysis of the proposed comprehensive strategy is shown in Figures 6–9.

From Figure 6a, when the active power drooping coefficient m_p varies from 0 to 1, the overall trend of the system root locus moves towards the right side with the increase of m_p , and reaches the right half plane eventually, and the system gradually loses its stability. Namely, the system becomes unstable if the m_p is too large. From Figure 6b, when the reactive power drooping coefficient n_q varies from 0 to 1, the overall trend of the system root locus moves towards the right side with the increase of n_q , and reaches the right half plane eventually, and the system gradually loses its stability. Namely, the system also becomes unstable if n_q is too large.

From Figure 7a, when m_{ph} varies from 0 to 1, the overall trend of the system root locus moves towards the right side with the increase of m_{ph} , and the system stability is weakened gradually. From Figure 7b, when n_{qh} varies from 0 to 1, the overall trend of the system root locus moves towards the right side with the increase of n_{qh} , and reaches the right half plane eventually, and the system stability is also weakened gradually.

Figure 8 shows the root locus of the proposed multi-inverter-based micro-grid system with comprehensive control strategy, which proves that all eigenvalues are located in the left half plane, meaning that the system controlled by the comprehensive strategy is stable.

In Figure 9, the root locus of the proposed comprehensive control strategy is represented by the red “•”, and the root locus of the conventional droop control strategy is represented by the blue “×”. The number of poles in the low frequency area of the proposed comprehensive control strategy is 13, and the conventional droop control strategy is 6 under the same parameters. The overall trend of the characteristic root of the proposed comprehensive control strategy is on the left side of the conventional droop control strategy, and the addition of three pairs of conjugate poles can enhance the rapidity of the system. The characteristic root of the proposed comprehensive control strategy and the conventional droop control strategy are all negative real roots, so the system is stable.

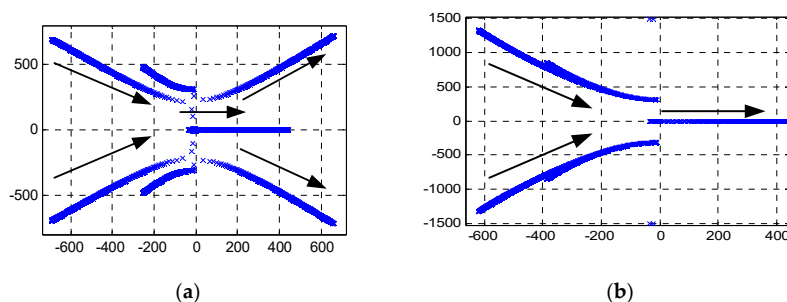


Figure 6. (a) The system root locus varies along with active power drooping coefficient m_p variation under fundamental frequency; (b) The system root locus varies along with reactive power drooping coefficient n_q variation under fundamental frequency.

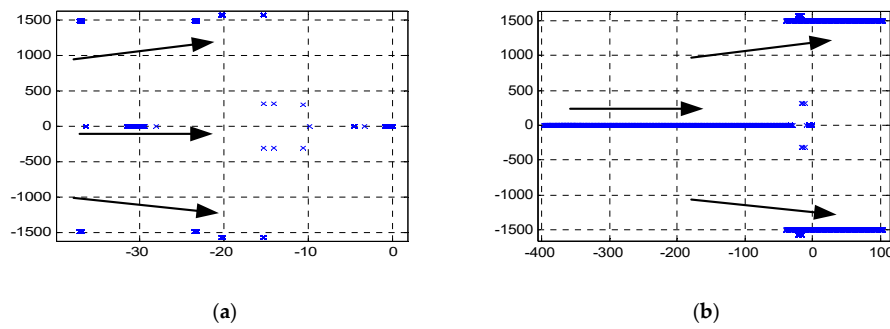


Figure 7. (a) The system root locus varies along with active power drooping coefficient m_{ph} variation under the h th harmonic frequency; (b) The system root locus varies along with reactive power drooping coefficient n_{qh} variation under the h th harmonic frequency.

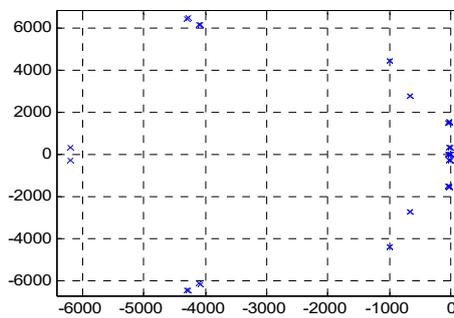


Figure 8. The root locus of the proposed multi-inverter-based micro-grid system.

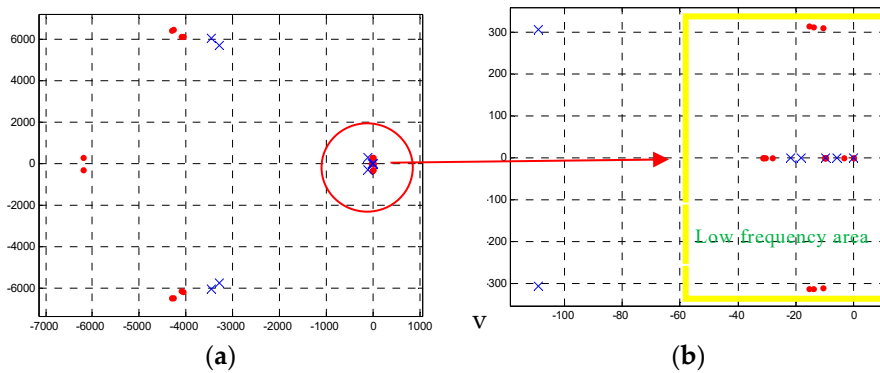


Figure 9. (a) The characteristic root contrast diagram of the proposed comprehensive control strategy and the conventional droop control strategy; (b) Part of the A graph is magnified.

4. Simulation Results

Simulations are built in MATLAB2014B, and the 5th, 7th, 11th, and 13th harmonics components are injected in the model. The simulation model is shown in Figure 10. The inverter output phase voltage amplitude is 311 V, and the frequency is 50 Hz. During simulations, the load fluctuates abruptly at 3 s, whose active power changes from 20 kW to 40 kW, and reactive power 0 kW to 20 kW. In order to verify the effectiveness of the proposed control strategy, the simulation analysis is carried out according to the following steps:

Step 1: the conventional droop control strategy of the micro-grid is simulated. The load is changed with different line impedances while the capacities of the inverters are the same, then the simulation results can be used as a reference for the following simulation.

Step 2: the comprehensive control strategy proposed in this paper is simulated and analyzed. The load is changed with different line impedances while the capacities of the inverters are the same.

Step 3: the proposed comprehensive control strategy is also proved with different inverters capacities, the load is changed in next simulations with different line impedances, while the capacity proportion of two inverters are 2:1.

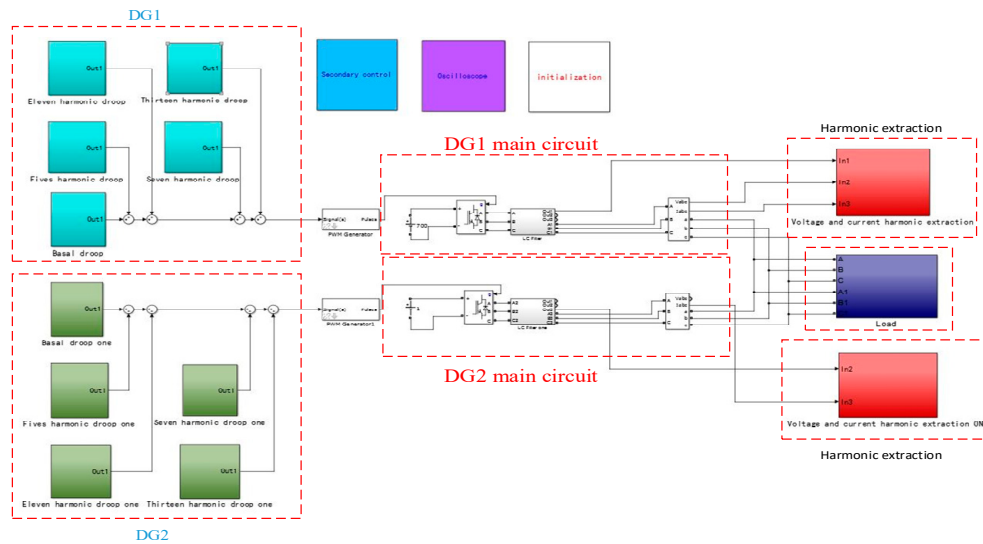


Figure 10. The simulation model in MATLAB2014B.

The simulation parameters used in this article are shown in Table 1.

Table 1. Information of simulation parameters.

Name	Parameter	Value	Parameter	Value	Parameter	Value
Main circuit	L_f	0.6×10^{-3} H	R_f	1×10^{-2} Ω	U_{ab}	700 V
	L_{line}	2.8×10^{-3} H	R_{line}	4.28×10^{-2} Ω		
Virtual impedance	R_{ref1}	2.14×10^{-3} Ω	R_{ref}	2.14×10^{-3} Ω	X_{ref1}	1.284×10^{-1}
	X_{ref2}	1.284×10^{-1}				
Fundamental wave droop control strategy	f^*	50 Hz	U^*	311 V	$m1:m2$	1:1
	$m1$	1×10^{-5}	$m2$	1×10^{-5}	$n1:n2$	1:1
	$n1$	3×10^{-5}	$n2$	3×10^{-5}	k_{up}	10
	k_{ui}	100	k_{ip}	5		
Harmonic wave droop control strategy	f^*	0 Hz	U^*	0 V	$m1:m2$	1:1
	$m1$	-1.361×10^{-2}	$m2$	-1.361×10^{-2}	$n1:n2$	1:1
	$n1$	2.609×10^{-2}	$n2$	-2.609×10^{-2}	k_{up}	10
	k_{ui}	50				

The results of the Step 1 simulations are shown in Figure 11.

From Figure 11a,b, the active powers of two inverters can be accurately distributed while the reactive powers cannot. The difference of reactive power between DG1 and DG2 is 7000 Var. In Figure 11c,d, the voltage and frequency fluctuate when the load changes. The values of voltage and frequency cannot be stabilized at 311 V and 50 Hz. The phase voltage reduction is 215 V, and the frequency reduction is 49.82 Hz. Meanwhile, the voltage waveform distortion in the 5th, 7th, 11th, and 13th harmonics are obvious. The 5th harmonic is 1.8%, 7th harmonic is 1.7%, 11th harmonic is 1.2%, and 13th harmonic is 0.7%.

The results of the Step 2 simulations are shown in Figure 12.

With the comprehensive strategy, the improvement of reactive power distribution is obvious in Figure 12b. In Figure 12c,d, the voltage and frequency can be stabilized at 311 V and 50 Hz while the load changes. The waveform has been significantly improved in Figure 12e, and the 5th, 7th, 11th,

and 13th harmonic components are suppressed in Figure 12f. The 5th harmonic is 0.02%, 7th harmonic is 0.02%, 11th harmonic is 0.01%, and 13th harmonic is 0.02%.

The results of the Step 3 simulations are shown in Figure 13.

The experimental results of simulation 3 are similar to those of simulation 2. The 5th, 7th, 11th, and 13th harmonics are almost completely eliminated by simulation 2 and simulation 3. The effect is shown in Table 2. There is no doubt that the proposed strategy is also effective for the system with different micro sources capacity proportions.

According to these three simulations, it can be seen that the comprehensive strategy this paper proposed can guarantee the accurate distribution of active power and reactive power between micro sources. The voltage and frequency can be stabilized at 311 V and 50 Hz while the load changes. Meanwhile, the 5th, 7th, 11th, and 13th harmonics components can be effectively suppressed. The effects of these three simulations are shown in Table 3.

Table 2. The 5th, 7th, 11th, and 13th harmonic variation test data.

Simulation Conditions	5th	7th	11th	13th	THD
Simulation 1	1.74%	1.61%	1.23%	0.74%	2.84%
Simulation 2	0.08%	0.13%	0.09%	0.02%	0.24%
Simulation 3	0.36%	0.24%	0.23%	0.02%	0.44%

Table 3. The contrast effects of different control strategy simulations.

Simulation Conditions	Simulation 1	Simulation 2	Simulation 3
Active power accurate distribution	No	Yes	Yes
Reactive power accurate distribution	No	Yes	Yes
Voltage and frequency stability of PCC while load changes	No	Yes	Yes
The 5th, 7th, 11th, and 13th harmonic suppression	No	Yes	Yes

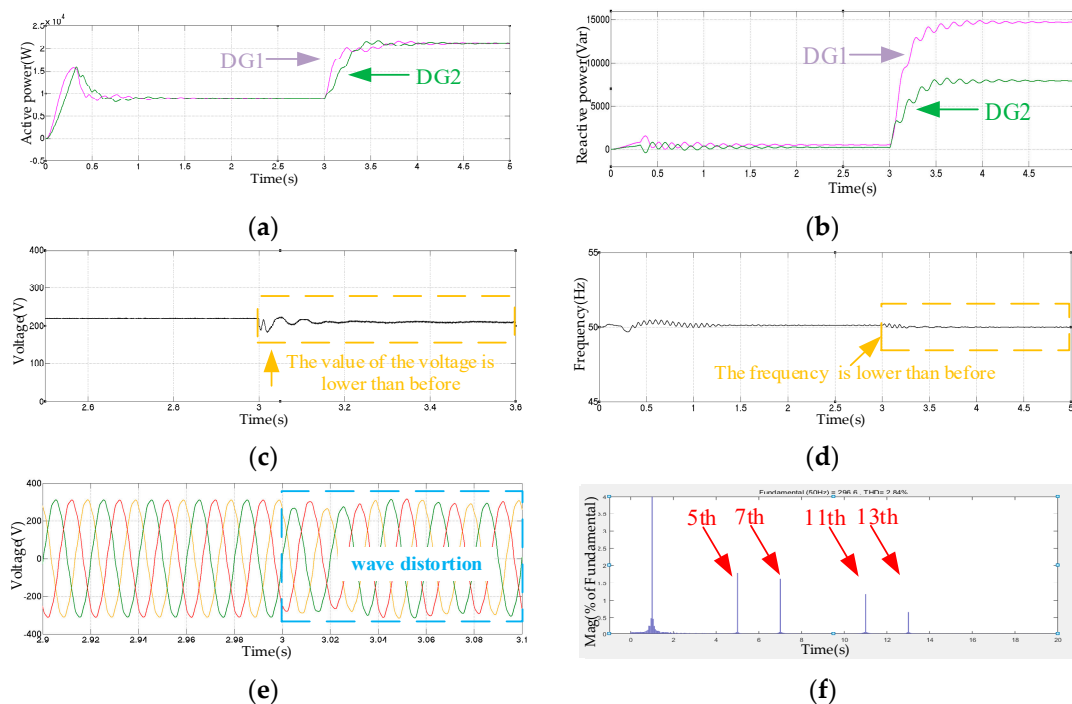


Figure 11. (a) Active power of DG1 and DG2 Inverters; (b) Reactive power of DG1 and DG2 Inverters; (c) The voltage value of PCC; (d) The frequency value of PCC; (e) Voltage waveform of PCC; (f) Voltage FFT analysis of PCC.

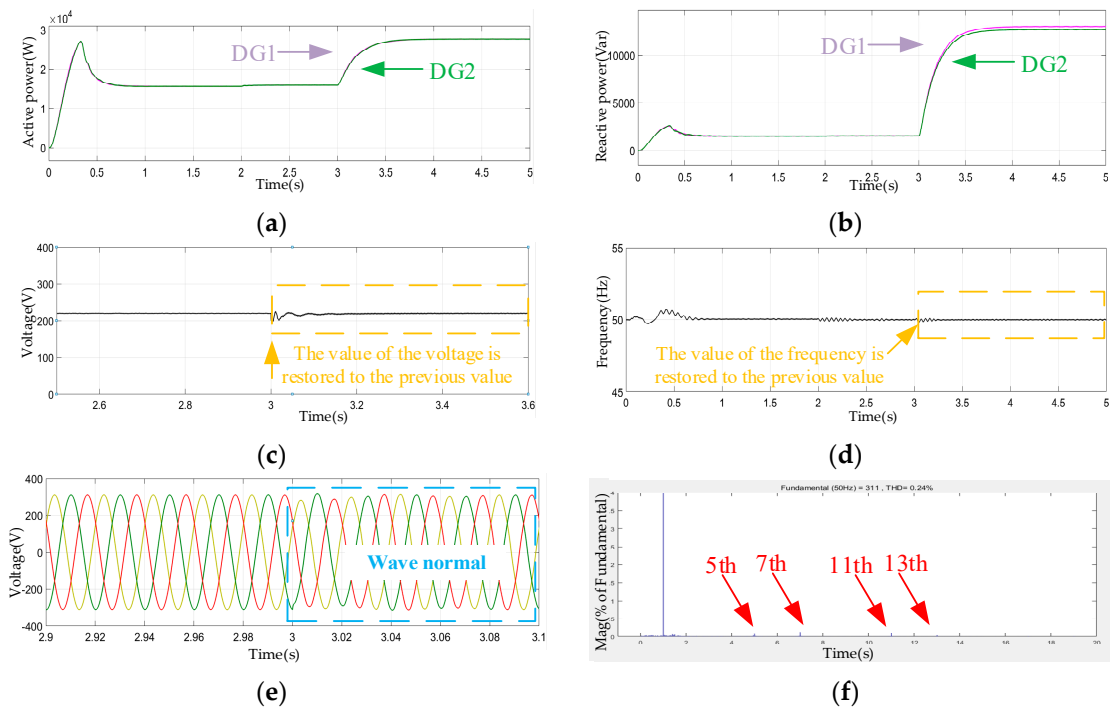


Figure 12. (a) Active power of DG1 and DG2 Inverters; (b) Reactive power of DG1 and DG2 Inverters; (c) The voltage value of PCC; (d) The frequency value of PCC; (e) Voltage waveform of PCC; (f) Voltage FFT analysis of PCC.

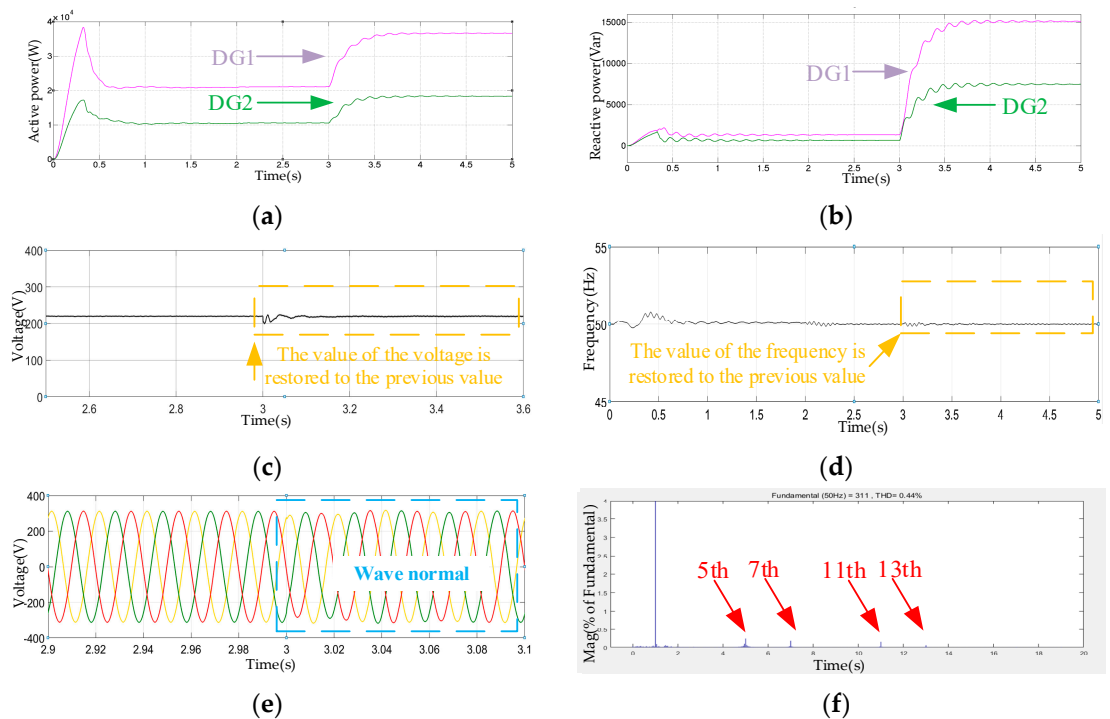


Figure 13. (a) Active power of DG1 and DG2 Inverters; (b) Reactive power of DG1 and DG2 Inverters; (c) The voltage value of PCC; (d) The frequency value of PCC; (e) Voltage waveform of PCC; (f) Voltage FFT analysis of PCC.

5. Conclusions

This paper proposes a comprehensive strategy for accurate reactive power distribution, stability improvement, and harmonic suppression of a multi-inverter-based micro-grid. With the combination of virtual impedance droop control and secondary power balance control, the active and reactive can be distributed accurately, meanwhile the stability of voltage and frequency are obviously improved. Next, a harmonic suppression control strategy is introduced to suppress harmonic components in the micro-grid. Furthermore, small signal analysis is used to analyze the stability of the proposed multi-converter parallel system after introducing the comprehensive theory. The results of MATLAB simulations certify that proposed the strategy has great performance on accurate reactive power distribution, stability improvement, and harmonic suppression.

More and more experts and scholars pay attention to the problems related to the power quality of the micro-grid. We will research on more projects related to the power quality of the micro-grid in the future, such as the power quality problems of the micro-grid with mixed loads and the transient problems of power quality in different operation modes.

Acknowledgments: This work was supported in part by the National Science and technology support project (2015BAA01B2) of China and Liaoning Electric Power Co., Ltd. science and technology project (2017YF-31) of State Grid.

Author Contributions: The paper was a collaborative effort among the authors. Henan Dong carried out relevant theoretical research, performed the simulation, analyzed the data, and wrote the paper. Shun Yuan and Zhiyuan Cai provided critical comments. Zijiao Han and Guangdong Jia performed the experiments. Yangyang Ge recorded the data.

Conflicts of Interest: The authors declare no conflict of interest.

References

1. Zhong, Q.C.; Hornik, T. *Control of Power Inverters in Renewable Energy and Smart Grid Integration*, 1st ed.; China Machine Press: Beijing, China, 2016; pp. 57–69, ISBN 978-7-11-154010-6.
2. Li, Y.; Feng, B.; Li, G.; Qi, J.; Zhao, D. Optimal distributed generation planning in active distribution networks considering integration of energy storage. *Appl. Energy* **2018**, *210*, 1073–1081. [[CrossRef](#)]
3. Zhao, B. *Key Technology and Application of Microgrid Optimal Configuration*, 1st ed.; Science Press: Beijing, China, 2015; pp. 154–196, ISBN 978-7-03-044745-6.
4. Hosseinzadeh, M.; Salmasi, F.R. Power management of an isolated hybrid AC/DC micro-grid with fuzzy control of battery banks. *IET Renew. Power Gener.* **2015**, *9*, 484–493. [[CrossRef](#)]
5. Hosseinzadeh, M.; Salmasi, F.R. Robust optimal power management system for a hybrid AC/DC micro-grid. *IEEE Trans. Sustain. Energy* **2015**, *6*, 675–687. [[CrossRef](#)]
6. Baghaee, H.R.; Mirsalim, M.; Gharehpetian, G.B.; Talebi, H.A. A decentralized power management and sliding mode control strategy for hybrid AC/DC microgrids including renewable energy resources. *IEEE Trans. Ind. Inf.* **2017**, *PP*. [[CrossRef](#)]
7. Li, D.; Zhao, B.; Wu, Z.; Zhang, L. An improved droop control strategy for low-voltage microgrids based on distributed secondary power optimization control. *Energies* **2017**, *10*, 1347. [[CrossRef](#)]
8. Zheng, Z.; Shao, W.H.; Zhao, W.F.; Ran, L.; Yang, H. Coordination control of multiple multi-functional grid-tied inverters to share power quality issues for grid-connected micro-grid. *Proc. CSEE* **2015**, *35*, 4947–4955.
9. Li, Y.; Li, Y.; Li, G.; Zhao, D.; Chen, C. Two-stage multi-objective OPF for AC/DC grids with VSC-HVDC: Incorporating decisions analysis into optimization process. *Energy* **2018**, *147*, 286–296. [[CrossRef](#)]
10. Hassan, M.; Ahmed, S.; Martin, J.P. Harmonic power sharing with voltage distortion compensation of droop controlled islanded microgrids. *IEEE Trans. Smart Grid* **2017**, *26*, 1949–1963.
11. Li, Y.W.; Kao, C.N. An accurate power control strategy for power-electronics-interfaced distributed generation units operating in a low-voltage multi-bus microgrid. *IEEE Trans. Power Electron.* **2009**, *24*, 2977–2988.
12. Lazzarin, T.B.; Bauer, G.A.T.; Barbi, I. A Control Strategy by Instantaneous Average Values for Parallel Operation of Single Phase Voltage Source Inverters Based in the Inductor Current Feedback. In Proceedings of the Energy Conversion Congress and Exposition, San Jose, CA, USA, 20–24 September 2009; pp. 495–502.

13. Jin, P.; Li, Y.; Li, G.; Chen, Z.; Zhai, X. Optimized hierarchical power oscillations control for distributed generation under unbalanced conditions. *Appl. Energy* **2017**, *194*, 343–352. [[CrossRef](#)]
14. Routimo, M.; Salo, M.; Tuusa, H. Comparison of voltage-source and current-source shunt active power filters. *IEEE Trans. Power Electron.* **2007**, *22*, 636–643. [[CrossRef](#)]
15. Grino, R.; Cardoner, R.; Costa-Castello, R.; Fossas, E. Digital repetitive control of a three-phase four-wire shunt active filter. *IEEE Trans. Power Electron.* **2007**, *54*, 1495–1503. [[CrossRef](#)]
16. Garcia-Cerrada, A.; Pinzon-Ardila, O.; Feliu-Batlle, V. Application of a repetitive controller for a three-phase active power filter. *IEEE Trans. Power Electron.* **2007**, *22*, 237–246. [[CrossRef](#)]
17. Costa-Castello, R.; Grino, R.; Parpal, C.R.; Fossas, E. High performance control of a single-phase shunt active filter. *IEEE Trans. Control Syst. Technol.* **2009**, *17*, 1318–1329. [[CrossRef](#)]
18. Ghosh, A.; Ledwich, G. A unified power quality conditioner (UPQC) for simultaneous voltage and current compensation. *Electron. Power Syst. Res.* **2001**, *59*, 55–63. [[CrossRef](#)]
19. Strzelecki, R.; Benysek, G. Power quality conditioners with minimum number of current sensors requirement. *Prz. Elektrotech.* **2008**, *11*, 295–298.
20. Sreekumar, P.; Khadkikar, V. A New Virtual Harmonic Impedance Scheme for Harmonic Power Sharing in an Islanded Microgrid. *IEEE Trans. Power Deliv.* **2016**, *31*, 936–945. [[CrossRef](#)]
21. Savaghebi, M.; Vasquez, J.C.; Jalilian, A.; Guerrero, J.M.; Lee, T.-L. Selective Harmonic Virtual Impedance for Voltage Source Inverters with LCL Filter in Microgrids. In Proceedings of the 2012 IEEE Energy Conversion Congress and Exposition (ECCE), Raleigh, NC, USA, 15–20 September 2012; pp. 1960–1965.
22. He, J.; Li, Y.W.; Guerrero, J.M.; Blaabjerg, F.; Vasquez, J.C. An islanding Microgrid power sharing approach using enhanced virtual impedance control scheme. *IEEE Trans. Power Electron.* **2013**, *28*, 5272–5282. [[CrossRef](#)]
23. Hamzeh, M.; Karimi, H.; Mokhtari, H. Harmonic and negative-sequence current control in an islanded multi-bus MV microgrid. *IEEE Trans. Smart Grid* **2014**, *5*, 167–176. [[CrossRef](#)]
24. Zhong, Q.C. Harmonic droop controller to reduce the voltage harmonics of inverters. *IEEE Trans. Ind. Electron.* **2013**, *60*, 936–945. [[CrossRef](#)]
25. Ananda, S.A.; Gu, J.C.; Yang, M.T.; Wang, J.M.; Chen, J.D.; Chang, Y.R.; Lee, Y.D.; Chan, C.M.; Hsu, C.H. Multi-Agent system fault protection with topology identification in microgrids. *Energies* **2016**, *10*, 28. [[CrossRef](#)]
26. Ren, B.Y.; Zhao, X.R.; Sun, X.D. Improved Droop Control Based Three-Phase Combined Inverters for Unbalanced Load. *Power Syst. Technol.* **2016**, *40*, 1163–1168.
27. Ziadi, Z.; Yona, A.; Senjyu, T. Optimal Scheduling of Voltage Control Resources in Unbalanced Three-Phase Distribution Systems. In Proceedings of the IEEE International Conference on Power and Energy, Kota Kinabalu, Malaysia, 2–5 December 2012; pp. 227–232.
28. Xiao, Z.; Li, T.; Huang, M.; Shi, J.; Yang, J.; Yu, J.; Wu, W. Hierarchical MAS based control strategy for microgrids. *Energies* **2010**, *3*, 8–9. [[CrossRef](#)]
29. Tu, C.M.; Yang, Y.; Xiao, F. The output side power quality control strategy for microgrid main inverter under nonlinear load. *Trans. China Electrotech. Soc.* **2017**, *32*, 53–62.
30. Guerrero, J.; Matas, J.; de Vicuna, L.G. Decentralized control for parallel operation of distributed generation inverters using resistive output impedance. *IEEE Trans. Ind. Electron.* **2007**, *54*, 994–1004. [[CrossRef](#)]

